

UNIFIED ELECTRONIC RECOMBINATION OF Ne-LIKE Fe XVII: IMPLICATIONS FOR MODELING X-RAY PLASMAS

Anil K. Pradhan and Sultana N. Nahar

Department of Astronomy, The Ohio State University, Columbus, OH 43210

Hong Lin Zhang

MS F663, Los Alamos National Laboratory, Los Alamos, NM 87545

Received _____; accepted _____

ABSTRACT

Unified recombination cross sections and rates are computed for $(e + \text{Fe XVIII}) \rightarrow \text{Fe XVII}$ including non-resonant and resonant (radiative and di-electronic recombination, RR and DR) processes in an ab initio manner with relativistic fine structure. The highly resolved theoretical cross sections exhibit considerably more resonance structures than observed in the heavy-ion storage ring measurements at Heidelberg, Germany. Nonetheless, the detailed resonance complexes agree well with experiment, and the unified rates agree with the sum of experimentally derived DR and theoretical RR rates to $\sim 20\%$, within experimental or theoretical uncertainties. Theoretical results may provide estimates of field ionization of rydberg levels close to the DR peak, and non-resonant background contributions, particularly close to the RR peak as $E \rightarrow 0$. More generally, the unified results avoid the physical and practical problems in astrophysical models inherent in the separation of electronic recombination into RR and DR on the one hand, and further subdivision into low-energy $\Delta n = 0$ DR and high-energy $\Delta n > 0$ DR in photoionized and collisionally ionized X-ray plasmas.

Subject headings: atomic data — atomic processes — line: formation — X-rays: general

1. INTRODUCTION

The *Chandra X-ray Observatory* and the *X-ray Multi-Mirror Mission - Newton* are observing a variety of sources (Canizares *et al.* 2000, Predehl *et al.* 2000) with wide-ranging plasma conditions. The analysis requires astrophysical models (e.g. Kallman 1995, Brickhouse *et al.* 1995) whose accuracy depend on the atomic cross sections for collisional and radiative processes such as electron impact excitation, photoionization and recombination. K- and L-shell iron ions are among the most prominent atomic species in many sources such as active galactic nuclei (Ogle *et al.* 2000), stellar coronae and winds (Schulz *et al.* 2000), and cooling flows in clusters of galaxies (Fabian *et al.* 2000). Excitation, photoionization, and recombination of Ne-like Fe XVII are of particular interest as this ion is a strong X-ray radiator owing to a multitude of L-shell excitations at $T < 1$ keV.

Although most of these atomic parameters are obtained theoretically, those need to be benchmarked against available experimental measurements. In recent years there has been considerable progress in both theoretical and experimental methods. High resolution electron-ion recombination measurements on ion storage rings show very detailed resonance structures in the low energy region usually accessible in experiments (e.g. Mannervik *et al.* 1997, Kilgus *et al.* 1992). Recently, such measurements have been done for $(e + \text{Fe XVIII}) \rightarrow \text{Fe XVII}$ (Savin *et al.* 1997, 1999) in the low energy region dominated by $\Delta n = 0$ resonances. The experimental results naturally measured the combined non-resonant and resonant contributions. These were then processed to separate the background and extract the resonance contributions (DR) by fitting with an experimentally deduced beam shape function. Savin *et al.* find that their inferred DR rates from low-energy measurements differ from previous theoretical calculations by up to a factor of 2 or more. Their best agreement of $\approx 30\%$ is with multi-configuration Dirac-Fock (MCDF) and Breit-Pauli (MCBP) calculations in the isolated resonance approximation, assuming autoionization

and the radiative probabilities independent of each other; detailed cross sections are not calculated. The comparison of derived DR rates from individual resonances (or blends) showed varying levels of agreement.

As the (e + ion) recombination is unified in nature, it is theoretically desirable to consider the non-resonant and resonant processes (RR and DR) together. A unified theoretical formulation has been developed (e.g. Nahar and Pradhan 1994, NP94; Zhang *et al.* 1999, Z99), including relativistic fine structure (Zhang and Pradhan 1997), and used to compute cross sections and rates for many atomic systems, such as the K-shell systems C IV - C V and Fe XXIV - Fe XXV of interest in X-ray spectroscopy (Nahar *et al.* 2000a,b; N99a,b). The unified results may be directly compared with experimental results, without the need to separate RR and DR. In this *Letter* we present new results for Fe XVII and show that not only are the unified cross sections and rates in very good agreement with experiment, but may also be used to study important physical effects such as ionization of high-rydberg bound and autoionizing levels. More generally, the results demonstrate that the unified calculations avoid the basic inconsistency and incompleteness of photoionization and recombination data for modeling of laboratory and astrophysical plasma sources.

2. THEORY AND COMPUTATIONS

From a quantum mechanical point of view photoionization and recombination may be treated in a self-consistent manner by considering the same coupled eigenfunction expansion for the core (photoionized or recombining) ion. For Fe XVII we write,

$$\Psi(E; e + Fe XVIII) = \sum_i \chi_i(Fe XVIII)\theta_i(e) + \sum_j c_j\Phi_j(Fe XVII), \quad (1)$$

where the Ψ denote both the bound ($E < 0$) and the continuum ($E > 0$) states of Fe XVII, expanded in terms of the core ion eigenfunctions $\chi_i(\text{Fe XVIII})$; the Φ_j are correlation functions. The close coupling approximation, based on the efficient R-matrix method (Burke *et al.* 1971), and its relativistic Breit-Pauli extension (Scott and Taylor 1981), enables a solution for the total Ψ , with a suitable expansion over the χ_i . The Breit-Pauli R-matrix (BPRM) method has been extensively employed for electron impact excitation under the Iron Project (Hummer *et al.* 1993, Berrington *et al.* 1995). The extension of the BPRM formulation to unified electronic recombination (e.g. Z99, N99a,b), and theoretically self-consistent calculations of photoionization and recombination is sketched below.

Resonant and non-resonant electronic recombination takes place into an infinite number of bound levels of the (e + ion) system. These are divided into two groups: (A) the low- n ($n \leq n_o \approx 10$) levels, considered via detailed close coupling calculations for photorecombination, with highly resolved delineation of autoionizing resonances, and (B) the high- n ($n_o \geq n \leq \infty$) recombining levels via DR, neglecting the background. In previous works (e.g. Z99) it has been shown that the energy region corresponding to (B), below threshold for DR, the non-resonant contribution is negligible. The DR cross sections converge on to the electron impact excitation cross section at threshold ($n \rightarrow \infty$, as required by unitarity, i.e. conservation of photon and electron fluxes. This theoretical limit is an important check on the calculations, and enables a determination of field ionization of rydberg levels of resonances contributing to DR.

Complete details of the extensive BPRM calculations for photoionization and recombination of Fe XVII will be presented elsewhere. The multi-configuration target eigenfunctions $\chi_i(\text{Fe XVIII})$ (Eq. 1) are obtained from an atomic structure calculation with 5 spectroscopic configurations $2s2p^5, 2s2p^6, 2s^22p^4 3s, 3p, 3d$, and a number of correlation configurations, optimized over the resulting 60 fine structure levels using the program

SUPERSTRUCTURE (Eissner *et al.* 1974). In the low energy region of interest in the present work, and experiment, the levels are $2s^2p^5$ (${}^2P_{1/2,3/2}^o$) and $2s2p^6$ (${}^2S_{1/2}$). The computed target level energies agree with the observed ones to $< 1\%$, and the oscillator strengths agree with those tabulated by NIST (<http://physics.nist.gov>) to $< 5\%$.

We consider photorecombination cross sections for 359 levels of Fe XVII. Total angular symmetries with $J \leq 7$ (odd and even), and levels with $\nu \leq 10.0$ (ν is the effective quantum number) are included in the photoionization calculations. The photorecombination cross sections are obtained via detailed balance using radiatively damped photoionization cross sections (Pradhan and Zhang 1997). Resonances with higher symmetries make negligible contribution. For $10 < \nu \leq \infty$ the calculations are carried out by extending the Bell and Seaton (1986) theory of DR. As the DR calculations are an extension of the electron scattering calculations (e.g. NP94,Z99), the DR and the electron impact cross sections are obtained in a self consistent manner satisfying the unitarity of the extended electron-photon S-matrix.

3. RESULTS

Fig. 1a shows the total unified recombination cross section σ_{RC} for Fe XVII. It shows photorecombination into all 359 levels of Fe XVII with $\nu \leq 10$ ($E \approx 90$ eV), and DR for $10 < \nu < \infty$ up to $E = 131.95$ eV, the ${}^2S_{1/2}$ threshold. A rydberg series of resonances converges on to the first excited level ${}^2P_{1/2}^o$ at 12.7 eV, followed by the stronger series $n \geq 6$ on the ${}^2S_{1/2}$ level at 131.95 eV. It is evident from Fig. 1a that the resonances complexes are highly resolved, the background contribution in the DR region is negligible. The resolution in σ_{RC} is remarkable given that it entails extremely detailed photoionization cross sections of hundreds of bound levels of Fe XVII. The cross sections have been radiatively damped;

the effect has been found to be much smaller than for H- and He-like ions (Pradhan and Zhang 1997, Z99). The resonance structures are resolved to convergence in the final rates. This required calculations at extremely fine energy meshes up to 10^{-4} eV for individual resonance complexes up to $n = 10$.

The nearly fully resolved cross sections exhibit considerably more detail than the beam-averaged cross sections in the experiment on the Heidelberg heavy-ion storage ring (Savin *et al.* 1999). For the illustrative comparison in Fig. 1b we convolve the theoretical $v \times \sigma_{RC}$ with a Gaussian of FWHM 0.020 eV. As the DR high- n resonances are extremely narrow we use an analytic average over the DR cross sections to obtain the rate coefficients in the region $10 < \nu \leq \infty$ below the $2s2p^6(^2S_{1/2})$ threshold. At low energies as $E \rightarrow 0$, the $\langle v * \sigma_{RC} \rangle$ in Fig. 1b are somewhat lower than the experimental values since the former include the non-resonant background up to $n \leq 10$, $J \leq 7$. However, the resonance complexes $n = 18 - 20$ (and higher) in the near-threshold region have been resolved (not shown for brevity), as in the inset in the lower panel showing experimental results. In the region $E < 12.7$ eV, the non-resonant RR-type contribution dominates the resonant DR-type contribution (see Fig. 2a and related discussion). Although the Gaussian tends to accentuate the peaks rather more sharply, the agreement in resonance heights, positions, and shapes of the $n = 6 - 10$ complexes appears generally quite good (different values of FWHM up to 0.050 eV produce little basic change). The experimental beam shape is simulated by a "flattened" Maxwellian function with velocity components transverse and parallel to the beam (e.g. Kilgus *et al.* 1992), which is then used to fit and extract 'resonance strengths' (Savin *et al.* 1999). While these may be compared with theory, a more precise comparison including the non-resonant background is now possible with the unified cross sections since the experiment also measures the same. But because the theoretical results are more detailed, and owing to extremely narrow widths of resonances, the precise beam shape function needs to be used for convolution as in experiment. However, the resonance

strengths may be compared independent of the beam shape function. For example, we find that the integrated cross section σ_{RC} for the $n = 7$ complex is $350.7 (10^{-21} \text{cm}^2 \text{eV})$, compared to the MCDF value 335.7 and experimental value of 412.0 ± 8.1 . More detailed comparisons will be presented in a later report.

As mentioned earlier, the peak of the DR cross section is theoretically equal to the threshold electron impact excitation cross section for the associated dipole core transition. The computed DR collision strength at the $^2S_{1/2}$ threshold is 0.27, in agreement with the electron impact excitation collision strength (Berrington and Pelan (2000) obtain 0.2882). The DR peak in Fig. 1b is shown with the experimentally determined field ionization cutoff at $n_{cut} \approx 124$; the $\langle v \times \sigma \rangle$ value is 3.87, compared to 4.18 at the theoretical limit at $n = \infty$, a difference of about 8%, indicating the degree of field ionization of the DR peak in the ion storage ring.

Of practical interest in astrophysical models is the total (e + ion) recombination rate coefficient $\alpha_R(T)$, including resonant and non-resonant (RR + DR) contributions, at all temperatures of ionic abundance. We present the maxwellian averaged $\alpha_R(T)$ in Fig.2, using the computed (unconvolved) σ_{RC} . Fig. 2a presents a partial $\alpha_R(T)$, including the unified σ_{RC} (Fig. 1), compared with the experimental DR results and the multi-configuration Dirac-Fock (MCDF) results (Savin *et al.* tabulate only the DR rates). The unified $\alpha_R(T)$ are significantly higher than the experimental DR-only rates because the non-resonant (RR-type) contribution monotonically rising towards low-T as $E \rightarrow 0$ is included, together with the DR bump around 0.4 eV due to the $^2P_{1/2} n \ell$ resonances. The experimental recombination cross sections also reflect these two features. The MCDF results are seen to underestimate DR.

Finally, Fig. 2b presents the total unified $\alpha_R(T)$ for Fe XVII (solid curve), using the calculated (unconvolved) cross sections, and including a "top-up" non-resonant background

contribution for recombination into rydberg levels $11 \leq n \leq \infty$ computed in the hydrogenic approximation (e.g. N99a,b). In order to compare precisely with experimental DR results, we fit and add to it the non-resonant background contribution from the present total σ_{RC} (Fig. 1a). The difference of $\sim 20\%$ between the unified α_R and this sum (‘Expt(DR) + non-resonant’) is then almost entirely due to DR. Also shown is the sum of experimental DR and the theoretical RR rate from Arnaud and Raymond (1992). Although a small contribution may still be unaccounted for, owing to resolution or high-partial waves, the unified and the experimental results are within theoretical or experimental uncertainties.

We also calculated DR via the forbidden $^2P_{3/2}^o - ^2P_{1/2}^o$ M1 core transition in Fe XVIII. Its contribution is negligible, although it may be of some consequence in other heavy, highly charged ions (Pradhan 1983) since $A(E2,M1)$ increases as much higher powers of Z than $A(E1)$.

4. DISCUSSION AND CONCLUSION

Astrophysical X-ray plasmas may be photoionized and/or collisionally ionized. Modeling of X-ray sources therefore requires total electronic recombination cross sections and rates at a wide range of energies and temperatures. To that end, we calibrate the unified theoretical and experimental data for recombination to Fe XVII against each other; we find good agreement in the low-energy region accessible experimentally. All other previous unified BPRM calculations have also shown very good agreement with experiments for few-electron recombined ions C IV, C V, O VII (Z99), Ar XIV (Zhang and Pradhan 1997), and Fe XXIV (Pradhan and Zhang 1997). Unified recombination cross sections including resonant and non-resonant processes (RR and DR) may therefore be computed for most astrophysically abundant elements.

In future, given the accuracy and resolution of the unified cross sections, and possible partial delineation according to n, ℓ , and J , an exact comparison with experimental measurements might yield precise information on: (i) the missing background non-resonant (RR) contribution near threshold as $E \rightarrow 0$, into high rydberg levels, (ii) extraneous background contribution such as due to charge transfer, and (iii) high rydberg resonances contributing to the DR peak, and a more accurate field ionization cut-off than the approximate formulae heretofore employed.

Whereas the detailed comparison with experiment (Fig. 1) for low-energy $\Delta n = 0$ ($E \leq 140$ eV) recombination is a useful test of accuracy, and relevant to low-T photoionized sources, collisionally ionized (coronal) high-T sources require total recombination rate coefficients up to $T = 10^8$ K (Arnaud and Raymond 1982). That, in turn, requires recombination cross sections up to $E \approx 1$ keV or higher. In fact, we may predict that the next DR peak at about 800 eV due to the $n = 3$ levels will be much bigger than at $^2S_{1/2}$ (Fig. 1), since there are several strong dipole transitions with A-values about 1-2 orders of magnitude higher than $A(^2S_{1/2} \rightarrow ^2P_{3/2,1/2}^o)$. The first set of these resonances begins at just above 400 eV, close to the temperature of maximum abundance of Fe XVII in coronal equilibrium. Correspondingly there will be a higher peak in the recombination rate than the one around 100 eV (Fig. 2). The $\Delta n = 1$ DR therefore is expected to contribute more to total electronic recombination of $(e + \text{Fe XVIII}) \rightarrow \text{Fe XVII}$ than the $\Delta n = 0$ core transitions. The higher energy unified recombination calculations are in progress.

One of the main points is that since photoionization and recombination are treated as inverse processes with the same eigenfunction expansion for the core ion (Eq. 1), the same set of resonances and non-resonant background are included in both processes - an essential requirement for self-consistency in photoionization equilibrium, as expressed by,

$$\int_{\nu_0}^{\infty} \frac{4\pi J_{\nu}}{h\nu} N(X^z) \sigma_{PI}(\nu, X^z) d\nu = \sum_j N_e N(X^{z+1}) \alpha_R(X_j^z; T), \quad (2)$$

where σ_{PI} is the photoionization cross section and J_ν the radiation flux. In general, the sum on the RHS of Eq. (2) extends over the infinite number of recombined bound levels. Now if the α_R on the RHS is subdivided into non-resonant RR and resonant DR, as in existing photoionization models, then fundamental inconsistencies result. The RR rate is supposedly derived from non-resonant photoionization cross sections. But as we see from Fig. 1, the near threshold region is dominated by resonances and a rising non-resonant background. Therefore, photoionization calculations must also be carried out including the same resonances (c.f. the Opacity Project work; Seaton *et al.* 1994, and references therein). There is however the issue of accurate resonance positions, which may be ameliorated by (a) averaging over the radiation field on the LHS of Eq. (2), and (b) pre-averaging over resonances in photoionization cross sections (Bautista *et al.* 1998). The further sub-division of DR into $\Delta n = 0$ rates (as, for example, derived experimentally by Savin *et al.* 1999) appropriate for only for low-T plasmas, and $\Delta n > 0$ DR needed in high-T plasmas, implies that the recombination rates must be obtained for (RR + DR ($\Delta n = 0$) + DR ($\Delta n > 0$)), generally using different approximations and possibly valid in different temperature regimes. These problems: (i) inconsistent photoionization and recombination, (ii) unphysical division of RR and DR, and (iii) low and high energy DR in different but overlapping energy(temperature) ranges, may be overcome with the unified method for electronic recombination, and corresponding photoionization cross sections, to enable a self-consistent treatment of photoionization and recombination in X-ray photoionized sources.

We would like to thank Dr. Werner Eissner for invaluable assistance with the BPRM codes. This work was partially supported by the NSF and the NASA Astrophysical Theory Program.

REFERENCES

- Arnaud, M. & Rothenflug, D. 1985, *A&AS* , 60, 425
- Bautista, M.A., Romano, P., & Pradhan, A.K. 1998, *ApJS*, 118, 259
- Bell, R.H. & Seaton, M.J. 1985, *Journal of Physics B: Atom. Molec. Opt. Phys.*, 18, 1589
- Berrington, K.A., Eissner, W., Norrington, P.H. 1995, *Comput. Phys. Commun.* 92, 290
- Berrington, K.A. & J. Pelan 2000, *A&A Suppl.*(submitted)
- Brickhouse, N., Raymond, J.C., & Smith, B.W. 1995, *ApJS*, 97, 551
- Burke, P.G., Hibbert, A. & Robb, D. 1971, *Journal of Physics B: Atom. Molec. Opt. Phys.*, 18, 1589
- Canizares, C.R. *et al.* in *Atomic data needs in X-ray astronomy* 2000, Eds. M.A. Bautista, T. R. Kallman & A.K. Pradhan, NASA Publications, NASA/CP-2000-209968 (www.heasarc.gsfc.nasa.gov/docs/heasarc/atomic/proceed.html)
- Eissner, W., Jones, M., & Nussbaumer, H. 1974, *Comput. Phys. Commun.* , 8, 270
- Fabian, A.C., Mushotzky, R.F., Nulsen, P.E.J. & Peterson, J.R. *MNRAS*(in press, astro-ph/0010509)
- Hummer D.G., Berrington K.A., Eissner W., Pradhan A.K, Saraph H.E., & Tully J.A., 1993, *A&A*, 279, 298
- Kallman, T. 1995, in *Atomic Processes in Plasmas*, AIP Press, New York (<http://heasarc.gsfc.nasa.gov/docs/heasarc/atomic/proceed.html>)
- Kilgus, G., Habs, D., Schwalm, D., Wolf, A., Badnell, N.R. & Müller, A. 1992, *Physical Review A*, 46, 5730

- Mannervik, S., Asp, S, Broström, L, DeWitt, D.R., Lidberg, L., Schuch, R. & Chung, K.T. 1996, *Physical Review A*, 55, 1810
- Nahar, S.N. & Pradhan, A.K. 1994, *Physical Review A*, 49, 1816 (NP94)
- Nahar, S.N., Pradhan, A.K. & Zhang, H.L. 2000a, *ApJS*(in press astro-ph/0003411); 2000b, *ApJS*(in press, astro-ph/0008023) (N99a,b)
- Ogle, P.M., Marshall, H.L., Lee, J.C. & Canizares, C.R. 2000 (in press, astro-ph/0010314)
- Predehl, P. *et al.* in *Atomic data needs in X-ray astronomy 2000*, Eds. M.A. Bautista, T. R. Kallman & A.K. Pradhan, NASA Publications, NASA CP-2000-209968
- Pradhan, A.K. & Zhang, H. L. 1997, *J. Phys. B* 30, L571
- Pradhan, A.K. 1983, *Physical Review A*, 28, 2128
- Savin, D.W, Bartsch, T., Chen, M.H., Kahn, S.M., Liedahl, D.A., Linkemann, J., Müller, A., Schippers, S., Schmitt, M., Schwalm, D. & Wolf, A. 1997, *ApJL*, 489, L115
- Savin, D.W., Kahn, S.M., Linkemann, J., Saghiri, A.A., Schmitt, M., Grieser, M., Repnow, R., Schwalm, D., Wolf, A., Bartsch, T., Brandau, C., Hoffknecht, A., Müller, A., Schippers, S., Chen, M. & Badnell, N.R. 1999, *ApJS*, 123, 687
- Schulz, N.S., Canizares, C.R., Husenmoerder, D, & Lee, J.C. *ApJL*(in press, astro-ph/0010310)
- Scott, N.S. & Taylor, K.T. 1982 *Comput. Phys. Commun.* , 25, 347
- Seaton, M.J., Yu Yan, Mihalas, D., & Pradhan, A.K. 1994, *MNRAS*, 266, 805
- Zhang, H.L. & Pradhan, A.K. 1997, *Phys.Rev.Lett*, 78, 195
- Zhang, H.L., Nahar, S.N. & Pradhan, A.K. 1999, *J. Phys. B*, 32, 1459 (Z99)

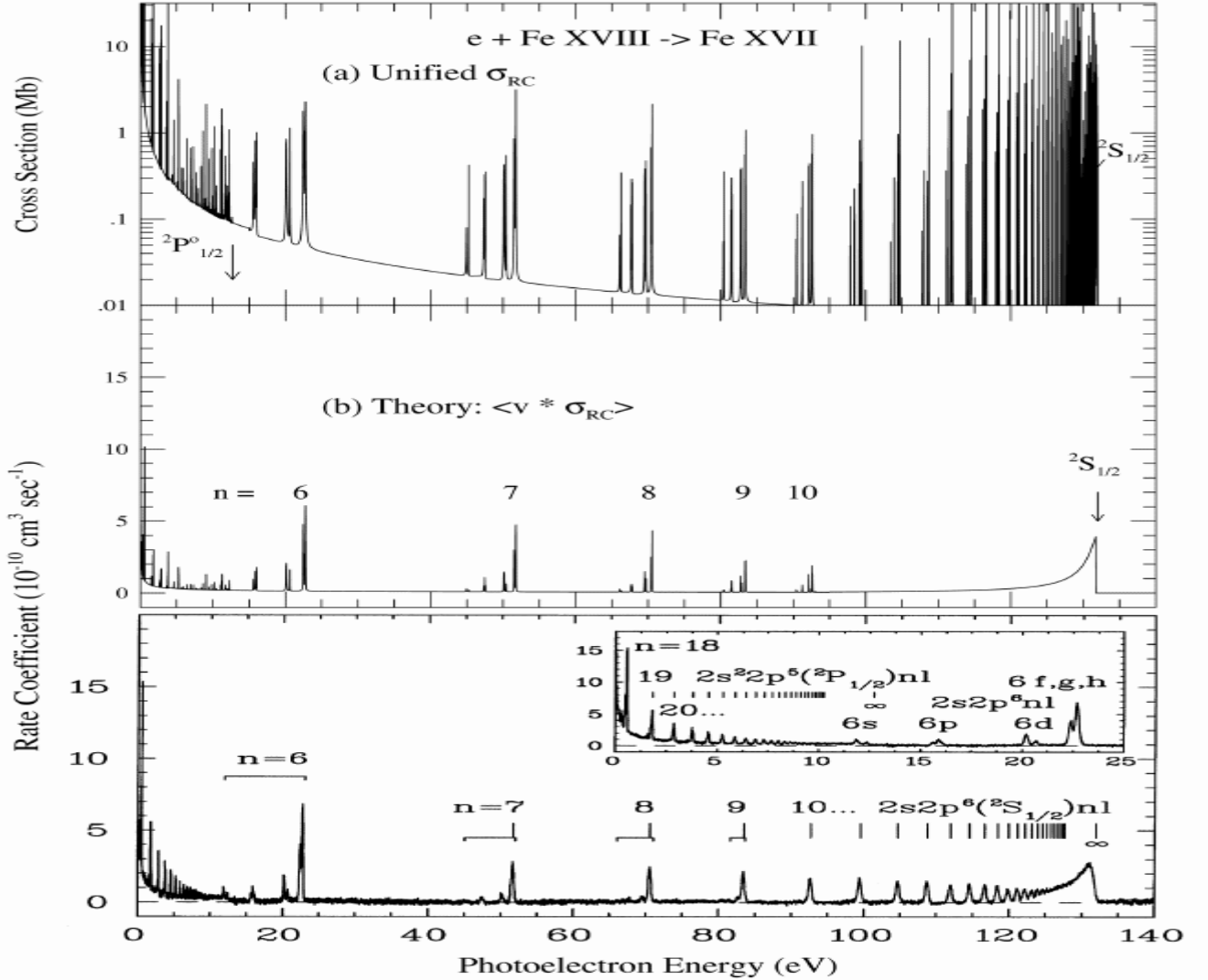


Fig. 1.— Unified recombination cross section σ_{RC} for Fe XVII: (a) Narrow rydberg resonances covering to the $2s^2 2p^5$ ($2P^o_{1/2}$) threshold at 12.7 eV, and the n-complexes belonging to the $2s 2p^6$ ($2S_{1/2}$) threshold are delineated. The high-n DR resonances are shown in the region $E > 90$ eV. (b) theoretical rate coefficients $\langle v \times \sigma_{RC} \rangle$ convolved over a gaussian beam shape, compared to experimental data in the lower panel (Savin *et al.* 1999). The theoretical DR resonances with $10 < \nu \leq \infty$ below the $2S_{1/2}$ threshold are analytically averaged.

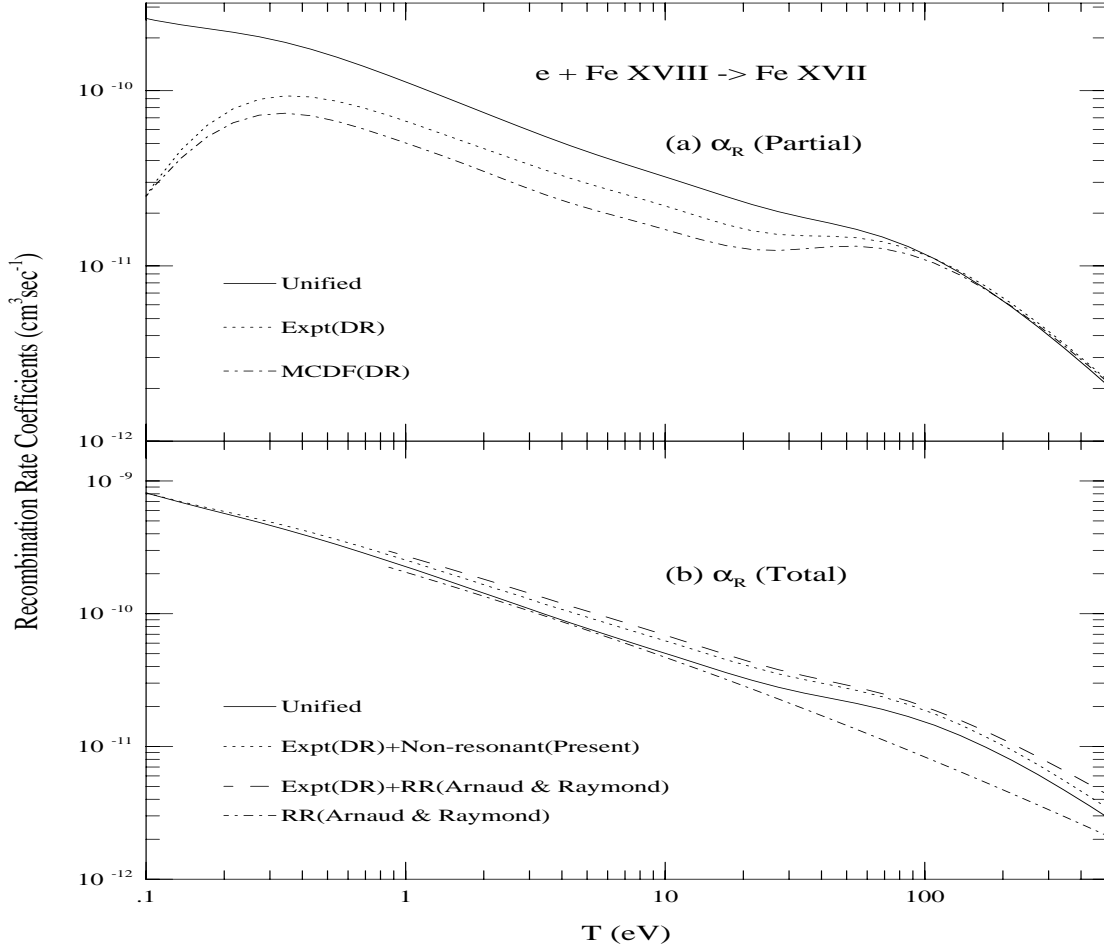


Fig. 2.— Unified recombination rate coefficients $\alpha_R(T)$ using computed σ_{RC} : (a) partial α_R corresponding to in Fig. 1, compared with the experimental DR-only rates and multi-configuration Dirac-Fock DR rates in Savin *et al.* (1999). The unified $\alpha_R(T)$ are significantly higher since they include the non-resonant background (including the low-T DR bump at ~ 0.4 eV); (b) the total $\alpha_R(T)$ compared with the sum of experiment (DR) and the present non-resonant background (RR-type). The agreement is $\sim 20\%$. Comparison with the sum of experiment (DR) and RR (Arnaud and Raymond) is also shown.